Solvent-free synthesis of luminescent copper(i) coordination polymers with thiourea derivatives

Solvent-free synthesis of luminescent copper(I) coordination polymers with thiourea derivatives

F. Grifasi,[†] M. R. Chierotti,[*,†] C. Garino,[†] R. Gobetto,[*,†] E. Priola,[†] E. Diana[†] and F. Turci[†]

[†] University of Torino, Department of Chemistry and NIS Centre of Excellence Via Pietro Giuria 7, 10125, Turin, Italy.

KEYWORDS. Thiourea, solid-state NMR, copper, luminescence, quantum yield.

ABSTRACT. This communication reports the solvent-free synthesis of a series of copper(I) cyanide (CuCN) based coordination polymers showing interesting luminescence properties and specific three-dimensional structures. The new compounds have been achieved by directly grinding CuCN together with thiourea (tu), N-methylthiourea (mtu), N-phenylthiourea (ptu), N,N'-diphenylthiourea (dptu) and 2,4-difluorophenylthiourea (fptu). The resulting compounds are: **$[(CuCN)_2(tu)]_n$**, **$[(CuCN)_5(mtu)_3]_n$**, **$[(CuCN)_3(mtu)_2]_n$**, **$[CuCN(ptu)]_n$**, **$[CuCN(dptu)]_n$** and **$[(CuCN)_3(fptu)_2]_n$**. "Seeding" crystallization was successful for **$[(CuCN)_2(tu)]_n$**, **$[CuCN(ptu)]_n$**, **$[CuCN(dptu)]_n$** and **$[(CuCN)_3(fptu)_2]_n$** and their structures have been resolved using X-Ray Single Crystal Diffraction. Owing to the microcrystalline powdered nature of compounds **$[(CuCN)_5(mtu)_3]_n$** and **$[(CuCN)_3(mtu)_2]_n$**, their characterization was mainly based on solid-state NMR, *via* ^{13}C CPMAS for ligand coordination and ^{1}H MAS for the weak interactions involving hydrogen atoms. Other solid-state techniques (Infrared Spectroscopy, X-

Ray Powder Diffraction, Differential Scanning Calorimetry and Thermo-Gravimetric Analysis) completed the characterization. Finally, the luminescence properties were explored by recording the emission and excitation spectra and also by evaluating the luminescence quantum yields and lifetimes. Such in-depth study gives promising results for the potential application as luminescent sensors of such compounds.

INTRODUCTION

Luminescent coordination polymers have been widely studied in recent decades and several new materials have been produced and tested.[1] In particular, the chemisorption of small molecules onto these materials has been shown to alter their luminescence properties,[2] prospecting potential applications as molecular sensing systems. In this context, copper(I) coordination polymers have not been as widely explored, if compared to other transition metal or lanthanide analogues.[3,4,5,6,7] In particular, CuCN can provide interesting luminescence properties when reacted with proper ligands. A recent computational study described its particular structure highlighting that, conversely to many inorganic salts forming 2D or 3D arrays, CuCN is characterized by 1D polymer chains consisting of two-coordinated metal centers and bridging cyano ligands.[8] CuCN itself is characterized by a weak luminescence.[9] However, its photoluminescence emission interestingly shifts from the near UV (392 nm) into the visible region upon the coordination of nucleophiles, while the intensity increases by several orders of magnitude. In some cases, small differences in the ligands, such as the presence of methyl or ethyl groups like in piperazine, methylpiperazine and ethylpiperazine, can result in remarkable differences in the emission color of the obtained coordination polymers, providing several luminescence tuning possibilities.[10]

Despite these promising properties, the real challenge over the last decade has been the optimization of the synthetic procedures using cheaper materials.[11] Great attention has been paid by chemists to the specific activity and selectivity of syntheses, with a special focus on the optimization of reagent use, by-product formation and purifying methods. This can be classified as a green chemistry approach, whose guidelines have been provided, although some controversy still abounds.[12] In this context, mechanochemistry has proven to be a groundbreaking approach, particularly useful in the preparation of new materials. It combines high success rate with low-cost, environmentally friendly procedures, products that may differ from those obtained *via* solution reactions, easy workup, short reaction time and high yields. This method is successfully applied in the field of crystal engineering, for example in cocrystal formation.[13] On the contrary, in the synthesis of coordination polymers and MOFs, solvothermal chemistry is the most common synthetic route.[14,15]

Our goal was to explore the luminescence properties of CuCN based coordination polymers employing a green chemistry approach founded on mechanochemical synthetic procedures. Moreover, particular attention was paid to address the following specific aims: 1) evaluation of the mechanochemistry efficacy in synthetizing coordination compounds with respect to traditional approaches; 2) structural characterization of the samples, even those obtained by means of mechanochemical methods which are usually in powdered microcrystalline form; 3) exhaustive study of the luminescence properties, carried out acquiring emission and excitation spectra and also measuring luminescence quantum yields and lifetimes which are key parameters to evaluate the possible application of the new materials as sensing devices.

In order to obtain luminescent compounds with emission in the visible region,[16] we combined CuCN with thiourea derivatives, directly grinding CuCN with thiourea (tu), N-

methylthiourea (mtu), N-phenylthiourea (ptu), N,N'-diphenylthiourea (dptu) and 2,4-difluorophenylthiourea (fptu) (**Scheme 1**). The ligands were chosen for their increasing steric hindrance in order to tune both the luminescence and porosity of the resulting compounds, namely **$[(CuCN)_2(tu)]_n$**, **$[(CuCN)_5(mtu)_3]_n$**, **$[(CuCN)_3(mtu)_2]_n$**, **$[CuCN(ptu)]_n$**, **$[CuCN(dptu)]_n$** and **$[(CuCN)_3(fptu)_2]_n$**. The traditional synthetic approach was also applied by using solvothermal/hydrothermal and crystallization methods. These compounds are rare cases of coordination polymers between bulky thioureas and copper salts, according to literature.[17] Moreover, no luminescence characterization is available for those already reported.

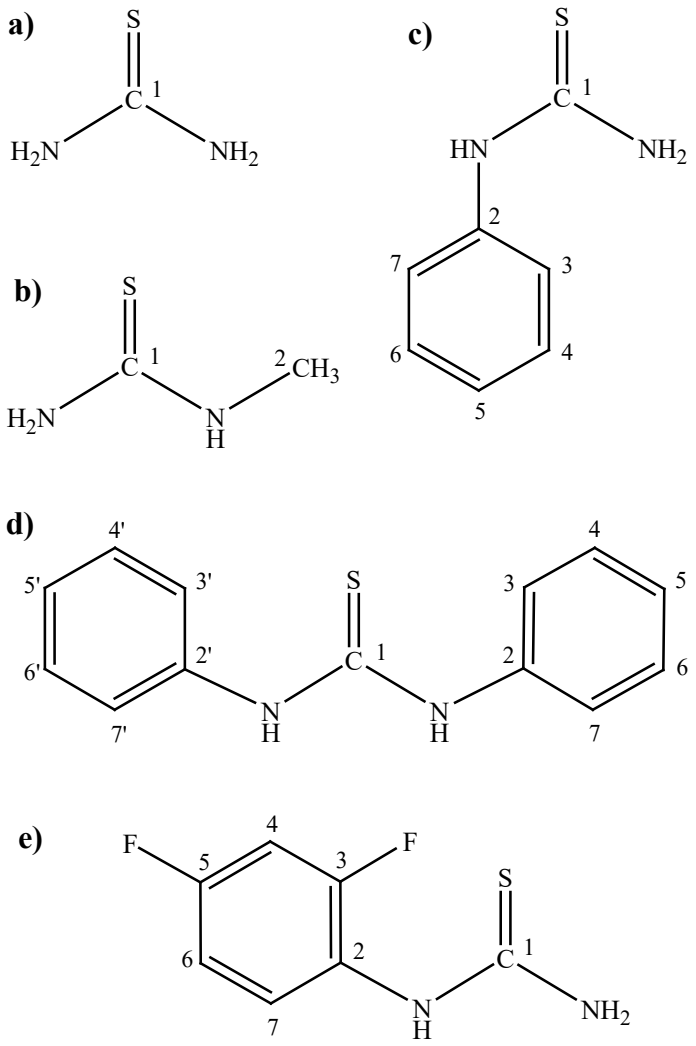

Scheme 1. Structures of ligands with atom number labelling: a) tu; b) mtu; c) ptu; d) dptu; e) fptu.

Owing to the powdered nature of the products, single crystals suitable for X-Ray Single Crystal Diffraction (XRSCD) analysis were only successfully obtained *via* seeding crystallization in the cases of **$[(CuCN)_2(tu)]_n$**, **$[CuCN(ptu)]_n$**, **$[CuCN(dptu)]_n$** and **$[(CuCN)_3(fptu)_2]_n$**. The structural characterization of the other compounds was achieved by means of Solid-State Nuclear Magnetic Resonance (SSNMR), X-Ray Powder Diffraction

(XRPD) and IR spectroscopy. In addition, calorimetric data were collected using Differential Scanning Calorimetry (DSC) and Thermo-Gravimetric Analysis (TGA). Luminescence properties were finally explored by means of emission, excitation, lifetime and quantum yield measurements, the latter being quite unusual for coordination polymers. Indeed, although almost no data have been found in literature, their measurements could open several applications.[18,19]

EXPERIMENTAL SECTION

Methods and materials. All reagents and solvents were purchased from Sigma Aldrich and used without further purifications. All samples were obtained *via* kneading *i.e.* grinding with a small quantity (0.2–2 ml) of solvent.[20,21,22] Hydrothermal/solvothermal techniques were also successfully applied. Crystals suitable for XRSCD were obtained by seeding crystallizations, that is by adding a "seed" (i.e. microcrystals obtained from either mechanochemistry or solvothermal reaction) in a stoichiometric saturated solution of the reagents.[23,24] **Table 1** summarizes synthesis and products.

$[(CuCN)_2(tu)]_n$: quantitative light grey powdered **$[(CuCN)_2(tu)]_n$** was obtained by kneading (100 µl of water or water/acetonitrile solution 1:1) CuCN (100 mg) and tu (85.0 mg), stoichiometric ratio 1:1, at room temperature for 16 hours using a mechanical ball-mill (Yield: 95%). It was also achieved by hydrothermal synthesis, *via* the dissolution of CuCN (400 mg), NaCN (221.4 mg) and tu (340 mg), in stoichiometric ratio 1:1:1, in 20 ml of water (100 °C, 6 hours) (Yield 45%): Grey needle shaped crystals, suitable for XRSCD, were collected after 48 hours of slow room temperature evaporation of a CuCN, NaCN and tu (1:1:1) water solution seeded with microcrystals from either kneading or solvothermal reaction. Elem. Anal. Calc. for

$C_3H_4N_4Cu_2S$: C, 14.12; H, 1.58; N, 21.95; Cu, 49.79%. Found: C, 14.04; H, 1.63; N, 21.83; Cu, 49.51%.

$[(CuCN)_5(mtu)_3]_n$: quantitative white powdered **$[(CuCN)_5(mtu)_3]_n$** was obtained *via* kneading (100 µl of water or water/acetonitrile solution 1:1) CuCN (100mg) and mtu (50.5 mg), stoichiometric ratio 1:1, at room temperature for 30 minutes with mortar and pestle (Yield: 96%). Elem. Anal. Calc. for $C_{11}H_{18}N_{11}Cu_5S_3$: C, 18.39; H, 2.53; N, 21.45; Cu, 44.24%. Found: C, 18.34; H, 2.55; N, 21.38; Cu, 44.10%.

$[(CuCN)_3(mtu)_2]_n$: quantitative light grey powdered **$[(CuCN)_3(mtu)_2]_n$** was obtained *via* hydrothermal synthesis, by dissolution of CuCN (400 mg), NaCN (221.4 mg) and mtu (202.0 mg), stoichiometric ratio 1:1:1, in 20 ml of water (100 °C, 6 hours) (Yield: 40%). Elem. Anal. Calc. for $C_7H_{12}N_7Cu_3S_2$: C, 18.73; H, 2.69; N, 21.84; Cu, 42.46%. Found: C, 18.64; H, 2.73; N, 21.73; Cu, 42.26%.

$[CuCN(ptu)]_n$: quantitative light grey powdered **$[CuCN(ptu)]_n$** was obtained *via* kneading (50 µl of water or water/acetonitrile solution 1:1) CuCN (100 mg) and ptu (85.2 mg), stoichiometric ratio 1:1, at room temperature for 25 minutes with a mortar and pestle (Yield: 98%). It was also achieved by solvothermal synthesis, by dissolution of CuCN (400 mg), NaCN (221.4 mg) and ptu (341.0 mg), stoichiometric ratio 1:1:1, in 20 ml of acetonitrile (80 °C, 6 hours) (Yield: 31%). Pale yellow prism shaped crystals, suitable for XRSCD, were collected after 48 hours of slow room temperature evaporation of a CuCN, NaCN and ptu (1:1:1) MeCN solution seeded with microcrystals from either kneading or solvothermal reaction . Elem. Anal. Calc. for $C_{16}H_{16}N_6Cu_2S_2$: C, 39.74; H, 3.33; N, 17.38; Cu, 26.28%. Found: C, 39.92; H, 3.38; N, 17.54; Cu, 26.01%.

[CuCN(dptu)]$_n$: quantitative light grey powdered **[CuCN(dptu)]$_n$** was obtained *via* kneading (50µl of ethanol or water/acetonitrile solution 1:1) CuCN (100 mg) and dptu (127.3 mg), stoichiometric ratio 1:1, at room temperature for 20 minutes with a mortar and pestle (Yield: 98%). It was also achieved by solvothermal synthesis, by dissolution of CuCN (400 mg), NaCN (221.4 mg) and dptu (511.4 mg), stoichiometric ratio 1:1:1, in 20 ml of acetonitrile (80 °C, 6 hours) (Yield: 41%). Pale yellow prism shaped crystals, suitable for XRSCD, were collected after 48 hours of slow room temperature evaporation of a CuCN, NaCN and dptu (1:1:1) MeCN solution seeded with microcrystals from either kneading or solvothermal reaction. Elem. Anal. Calc. for $C_{14}H_{12}N_3CuS$: C, 52.90; H, 3.8; N, 13.22; Cu, 19.99%. Found: C, 52.71; H, 3.83; N, 13.17; Cu, 19.92%.

[(CuCN)$_3$(fptu)$_2$]$_n$: quantitative light grey powdered **[(CuCN)$_3$(fptu)$_2$]$_n$** was obtained *via* kneading (50µl water or water/acetonitrile solution 1:1) CuCN (100mg) and fptu (105.1 mg), stoichiometric ratio 1:1, at room temperature for 30 minutes with mortar and pestle (Yield: 98%). It was also achieved by solvothermal synthesis, by dissolution of CuCN (400 mg), NaCN (221.4 mg) and thiourea(420.2 mg), stoichiometric ratio 1:1:1, in 20 ml of acetonitrile (80 °C, 6 hours) (Yield: 50%). Colorless prism shaped crystals, suitable for XRSCD, were collected after 48 hours of slow room temperature evaporation of a CuCN, NaCN and fptu (1:1:1) MeCN solution seeded with microcrystals from either kneading or solvothermal reaction. Elem. Anal. Calc. for $C_{17}H_{12}N_7Cu_3S_2F_4$: C, 31.65; H, 1.87; N, 15.2; Cu, 29.55%. Found: C, 31.82; H, 1.91; N, 15.32; Cu, 29.37%.

Suitable single crystals of **[(CuCN)$_2$(tu)]$_n$**, **[CuCN(ptu)]$_n$**, **[CuCN(dptu)]$_n$** and **[(CuCN)$_3$(fptu)$_2$]$_n$** were mounted on a Gemini R Ultra diffractometer.[25] The diffraction data were collected at 293(2) K using graphite-monochromated Mo-Kα radiation (λ= 0.71073 Å). The

orientation matrix and lattice parameters were obtained by least-squares refinement of the reflections obtained by a θ-χ scan (Dirax/lsq method). Data collection and reduction were performed using the CrysAlisPro[26] program. Numerical absorption correction was carried out using the CrysAlisAbs pack program. All measured reflections were used in the analysis. The structures were resolved using direct methods and refined with the full matrix least squares technique on F^2 using the SHELXS-97 and SHELXL-97 programs.[27] All non-hydrogen atoms were refined anisotropically. The hydrogen atoms were set in geometrical positions and refined using a riding model. **[(CuCN)$_2$(tu)]$_n$** and **[CuCN(ptu)]$_n$** occur in chiral space groups, in $P2_1$ and in $P2_12_12_1$, respectively (**Figure 1** and **2**). **[CuCN(dptu)]$_n$** and **[(CuCN)$_3$(fptu)$_2$]$_n$** occur in monoclinic C2/c and in centrosymmetric P-1 space groups, respectively (**Figure 3** and **4**). The Flack parameter[28,29] allowed us to assign the correct enantiomer. The refinement of the other possible enantiomer gave worse results in terms of R parameters, thus the enantiomer with the lower R values is reported. End-for-end disorder of CN groups is usually found in copper(I) cyanide compounds. For this reason, such groups were refined using the degree of disorder as a variable. Ordered arrays of cyanide were found in both structures.

[CuCN(dptu)]$_n$ presents substitutional disorder in cyanide positions, but the presence of a 2 symmetry axis constrains the nitrogen and carbon percentage at 50 % each. Despite the low crystalline quality of this compound, owing to small crystals dimensions and deliquescence, the results are sufficiently accurate for the analysis. The structure of **[(CuCN)$_3$(fptu)$_2$]$_n$** was refined from data collected on a non merohedral geminated crystal, but the non-overlapping reflections were sufficient to obtain a good refinement. A summary of the crystallographic data, structure refinement, selected bond distances and angles for **[(CuCN)$_2$(tu)]$_n$**, **[CuCN(ptu)]$_n$**, **[CuCN(dptu)]$_n$**, and **[(CuCN)$_3$(fptu)$_2$]$_n$** is given in **Table S1** of the Supporting Information. The

asymmetric units, with labels and the thermal ellipsoids derived from anisotropic refinement, are reported in **Figure S1** of the Supporting Information. Crystallographic information is deposited in the CCDC database with numbers 1044518-1044519-1044520-1044521.

X-ray Powder Diffraction patterns were collected on a PW1830/X'Pert PRO MPD diffractometer from PANalytical working in the Bragg-Brentano geometry, using the high-powered ceramic tube PW3373/10 LFF with a Co anode focused by a PW3152/63 X-ray mirror as a source. Powdered samples were placed inside a polymeric sample holder. All XRPD patterns and the comparison between calculated and experimental patterns are reported in **Figure S2** and **S3** in the Supporting Information, respectively.

All solid-state NMR spectra were recorded on a Bruker Avance II 400 instrument operating at 400.23 and 100.65 MHz for ^{1}H and ^{13}C nuclei, respectively. 4 mm o.d. zirconia rotors (sample volume of 80 μL) were employed and spun at 12 kHz for ^{13}C CPMAS spectra. A ramp cross-polarization pulse sequence was used with contact times of 3–5 ms, a ^{1}H 90° pulse of 3.8 μs, recycle delays of 1–60 s and 48–4096 transients. ^{1}H MAS spectra were performed on a 2.5 mm probe with a spinning speed of 32 kHz. A DEPTH sequence (π/2–π–π) was used to suppress the probe background signal.[30,31] The ^{1}H 90° pulse length was set to 2.50 μs, the recycle delays to 1–40 s and 32–64 transients were averaged for each sample. ^{1}H and ^{13}C chemical shifts were referenced through the resonance of adamantane (^{1}H signal at 1.87 ppm) and hexamethylbenzene (^{13}C methyl signal at 17.4 ppm), respectively.

Infrared-Attenuated Total Reflectance (IR-ATR) spectra were collected using a Harrick MVP2 ATR cell with a Bruker FT-IR Equinox 55 equipped with KBr optics and a DLaTGS detector. The spectra were acquired at 4 cm^{-1} resolution over 16–32 scans.

Differential Scanning Calorimetry (DSC) analyses were performed on a TA instrument Q200. The samples (5–10 mg) were placed in sealed alumina pans and heated at a rate of 10 °C·min^{-1} (temperature range: 50–400 °C). Thermogravimetric (TGA) measurements were performed under N_2 flow at a heating rate of 10 °C·min^{-1} (temperature range: 50–500 °C) on a TA instrument Q600 SDT Simultaneous DSC-TGA heat flow analyzer. The samples (5–10 mg) were placed in alumina pans.

Solid-state emission and excitation spectra together with luminescence lifetimes and quantum yields were acquired at room temperature using a HORIBA Jobin Yvon IBH Fluorolog-TCSPC spectrofluorimeter equipped with a Quanta-φ integrating sphere. Luminescence lifetimes were determined by time-correlated single-photon counting. Excitation *via* nanosecond pulses of 270 nm light generated by a NanoLED pulsed diode was used. All the emission data were collected using the same spectral bandwidth of 2–2 nm. Data were collected into 2048 channels to 10000 counts in the peak channel. Emission decay data were analyzed using the software DAS6 (TCSPC Decay Analysis Software).

Elemental analysis was performed on a CHN analyzer (CE Instruments, NA2100 Protein; after a pre-treatment in a furnace at 100 °C for 4 hours) and atomic absorption spectrometer (AAnalyst 400 Perkin Elmer, for Cu determination) for all compounds. The data confirm the stoichiometries deducted by XRSCD of **$[(CuCN)_2(tu)]_n$**, **$[CuCN(ptu)]_n$**, **$[CuCN(dptu)]_n$** and **$[(CuCN)_3(fptu)_2]_n$**. For **$[(CuCN)_5(mtu)_3]_n$** and **$[(CuCN)_3(mtu)_2]_n$** the experimental data have been confirmed by C/N ratio deducted from SSNMR. Data are reported in the Experimental section.

RESULTS AND DISCUSSION

All the coordination polymers were prepared using two synthetic approaches: the mechanochemical technique and the solvothermal/hydrothermal one. It is worth noticing that the kneading technique provides almost quantitative yields (from 95 to 98%) while the solvothermal/hydrothermal approach gives yields around 30–50% (**Table 1**). Moreover, reacting CuCN and mtu, the mechanochemical and solvothermal approaches lead to different compounds: **$[(CuCN)_5(mtu)_3]_n$** and **$[(CuCN)_3(mtu)_2]_n$**, respectively.

The characterization of all the compounds was carried out by means of SSNMR, XRPD, IR-ATR, DSC-TGA, DR-UV-Vis and emission spectroscopy.

Table 1. Summary of the syntheses involving CuCN and thioureas *via* mechanochemistry and solvothermal synthesis.

Reagents		Preparation	Formula	Yield
CuCN	tu	k (H_2O; r.t.; 16 h)	**$[(CuCN)_2(tu)]_n$**	95
		h (acq. sol. NaCN saturated; 100 °C; 6 h)		45
CuCN	mtu	k (H_2O; r.t.; 30 min.)	**$[(CuCN)_5(mtu)_3]_n$**	96
CuCN	mtu	h (acq. sol. NaCN saturated; 100 °C; 6 h)	**$[(CuCN)_3(mtu)_2]_n$**	40
CuCN	ptu	k (H_2O; r.t.; 25 min.)	**$[CuCN(ptu)]_n$**	98
		s (sol. MeCN, NaCN saturated; 80 °C; 6 h)		31
CuCN	dptu	k (H_2O; r.t.; 20 min.)	**$[CuCN(dptu)]_n$**	98
		s (sol. MeCN, NaCN saturated; 80 °C; 6		41
CuCN	fptu	k (H_2O; r.t.; 30 min.)	**$[(CuCN)_3(fptu)_2]_n$**	98
		s (sol. MeCN, NaCN saturated; 80 °C; 6		50

k: kneading; h/s: hydrothermal/solvothermal synthesis.

Single Crystal X Ray Diffraction. The structure of **$[(CuCN)_2(tu)]_n$** can be described as a 3D coordination polymer built of bridging cyanide and tu (**Figure 1a**). Only a few other copper(I) 3D polymers are reported with this family of ligands, none of which has a cyanide anion.[32,33]

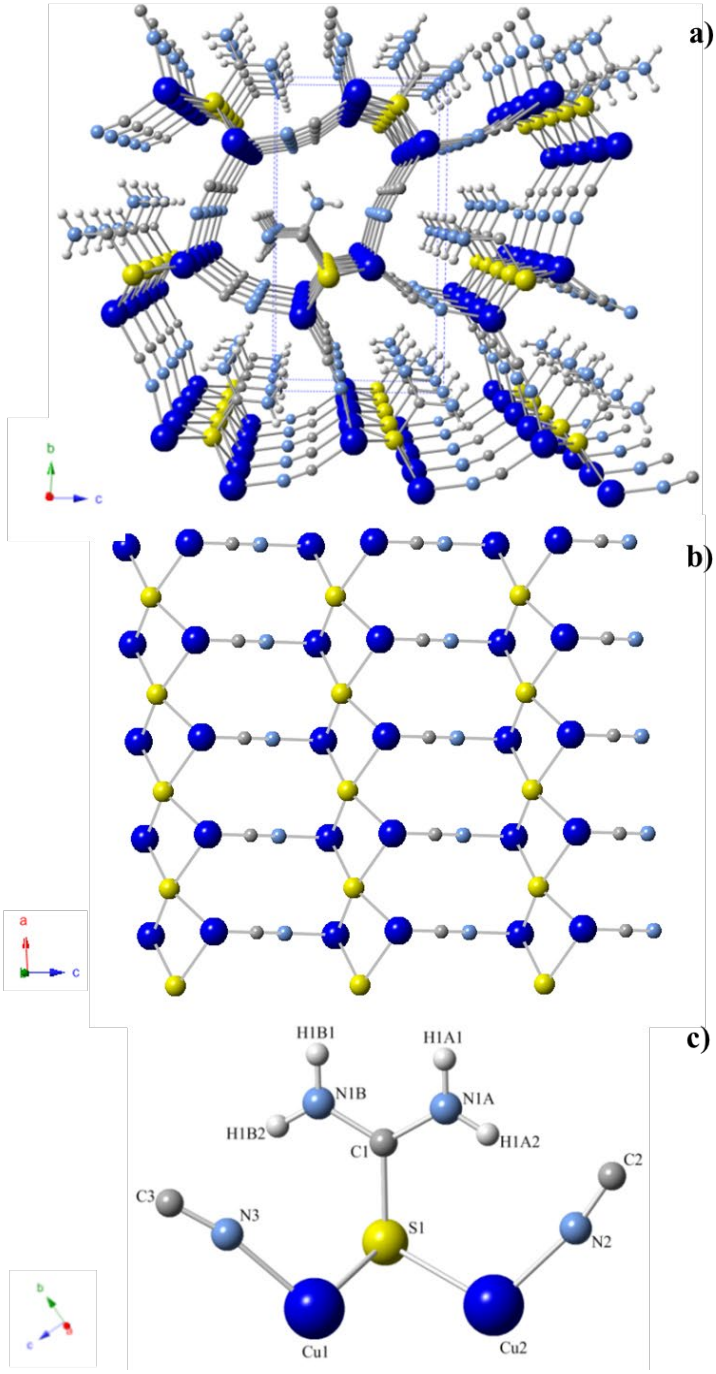

Figure 1. XRSCD structure of **$[(CuCN)_2(tu)]_n$**: **a)** packing, viewed along the a axis; **b)** structure of the layer formed by copper ions in (101) plane (H, C and N atoms of tu omitted for clarity); **c)** asymmetric unit.

This is in agreement with literature data, where high dimensional structures are generated by low CuX:tu ratios and less substituted tu.[34,35,36,37,38] The structure is characterized by two independent distorted tetrahedral Cu(I) ions, which form a layer in the (101) plane based on Cu_2S_2 parallelograms and $Cu_4S_2CN_2$ hexagonal metallocycles (**Figure 1b**). The Cu_2S_2 ring is typical of this family of complexes,[39] with a peculiar lozenge geometry (i.e. alternating long and short bridging Cu–S distances) consequent to the nature of the bridging S orbitals and electrons. The S–Cu–S and Cu–S–Cu angles, 90.96(6)° and 74.65(7)° respectively, are typical of this kind of structure. The observed Cu1–Cu2 distance [3.152(1)Å] suggests the absence of metal-metal interactions due to the open arrangement of the lozenge geometries.[40,41] The ligand shows a rare μ_4 coordination mode that, to the best of our knowledge, has been found in copper(I) chemistry with unsubstituted tu for the first time. Other examples, with substituted tu or other d^{10} metals, are $[Cu_4(L)_9](NO_3)_4 \cdot 6H_2O$ (L: N-ethylthiourea)[42] and $(AgBr)_2tu_3$,[43] respectively. The μ_4-thioamide ligand connects four Cu–CN–Cu chains, running along the b axis (the 2_1 axis), which are parallel to each other. This feature is typical of CuCN architectures in 2D coordination $(CuCN)_3(L)_2$ (L: N,N'-dimethylthiourea) and $(CuCN)_2(L)$ (L: N-ethylthiourea) polymers,[17] and differs from the behavior of silver(I) cyanide coordination polymers where the CN ligand is mainly terminal. All tu hydrogen atoms are involved in hydrogen bonds with the CN nitrogen (**Figure 1a**) (donor-acceptor distance: N1B–N3': 3.004(8) Å, N1A–N2: 3.187(8) Å, N1B–N2': 3.243(8) Å, N1A–N3": 3.292(8) Å). These interactions prevent the possible disorder of the CN groups in the refinement.

$[CuCN(ptu)]_n$ is a ladder polymer along the a axis (corresponding to the 2_1 axis of the space group), formed by parallel Cu–CN–Cu chains bridged by μ_2-ptu ligands (**Figure 2**).

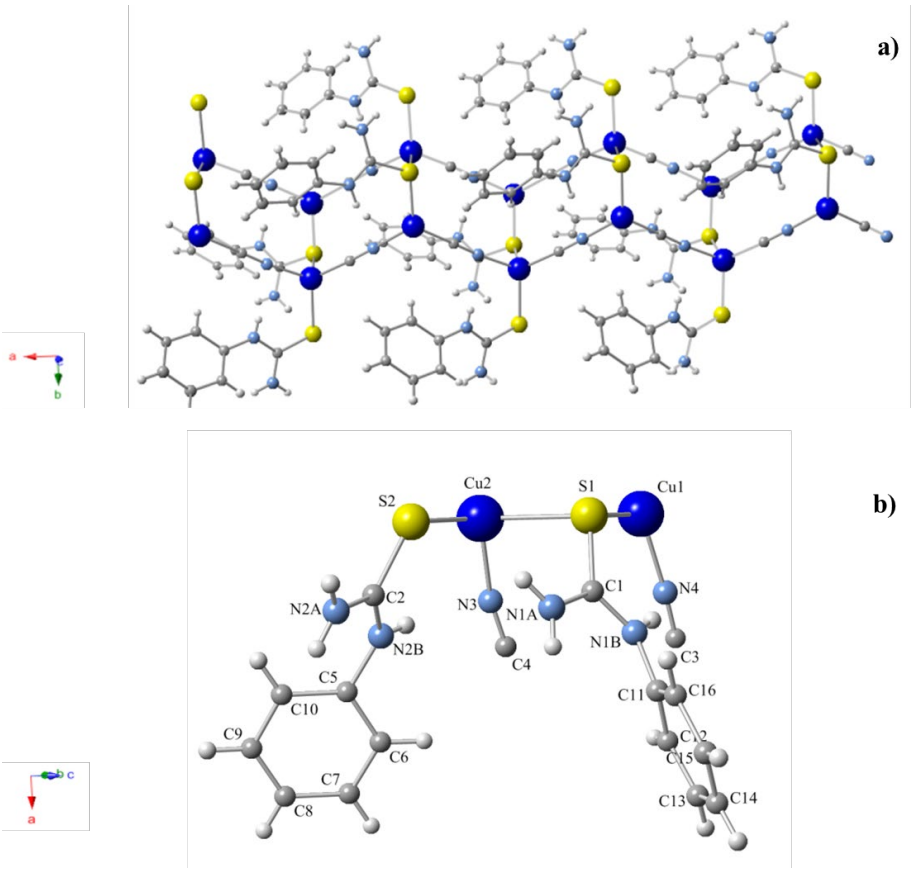

Figure 2. XRSCD structure of **[CuCN(ptu)]$_n$**: **a)** 1D coordination polymer along a axis (hydrogen atoms omitted for clarity); **b)** asymmetric unit.

This is the second known example of a complex between ptu and CuX salts.[44] The asymmetric unit presents two non-equivalent copper(I) ions, namely Cu1 in a trigonal planar environment (CNS) and Cu2 in a tetrahedral coordination (CNS_2), with a bridging ptu and another one in a terminal position. A similar polymer has already been reported for (CuCN)(L) (L: tetramethylthiourea), showing two polymorphs,[17] whereas an opposite situation was observed in $(CuCN)_3(L)_2$ (L: N,N'-dimethylthiourea), in which the cyanide acts as a bridge between the two metallic chains formed by μ_2-tetramethylthiourea ligands.[17]

The bridging ptu displays asymmetric bond lengths with the two non-equivalent copper(I) ions (S1–Cu1: 2.296(1) Å, S1–Cu2: 2.538(1) Å). The measured Cu1-Cu2 distance [3.617(1) Å], coupled to a Cu–S–Cu angle of 96.75(2)°, rules out presence of any feasible metal-metal interactions. The torsion angles to the tu frameworks of the two non-equivalent ptu phenyl rings are 45.03(2)° and 43.44(3)° respectively, the smallest values found in literature. This indicates that conjugate effects between the C=S bond and the benzene ring are absent. A hydrogen bonding network connects the parallel chains, consisting of two types of H-bonds: i) N–H···S, between two ptu from different chains [S1'···N2A: 3.496(2) Å and S2'···N1A: 3.547(2) Å, symmetry codes for S1' and S2'][45] and ii) N–H···N between ptu and CN of the same chain [N2B···N3: 3.045(3) Å, N1B···N4: 3.108(3) Å]. Presence of this H-bond network explains the lack of disorder in the cyanide groups.

[CuCN(dptu)]$_n$ has a monoclinic structure in which a planar trigonal copper centre is bound to two cyanide ligands and to a terminal dptu ligand(**Figure 3**). The two phenyl rings form torsional angles of 115.3(2)° and 55.6(2)° with respect to C2–N2A and C2–N2B bonds respectively, indicating the absence of interactions between the aromatic rings and the CS double bond. The copper(I) units are bound through the cyanides, forming a chain along the c axis (where the c glide plane is). The organic ligands, in trans-conformation, are located along the Cu–CN–Cu chain stabilizing the structure with van der Waals interactions. This polymeric behavior is similar to that observed in the derivative of tetramethylthiourea, CuCN(L) (L: tetramethylthiourea).[17] Due to its significant steric hindrance, **[CuCN(dptu)]$_n$** represents a rare occurrence of a dptu ligand polymeric structure with a d^{10} metal salt. To the best of our knowledge, the only other known case is Cd $(SCN)_2(dptu)_2 \cdot H_2O$.[46]

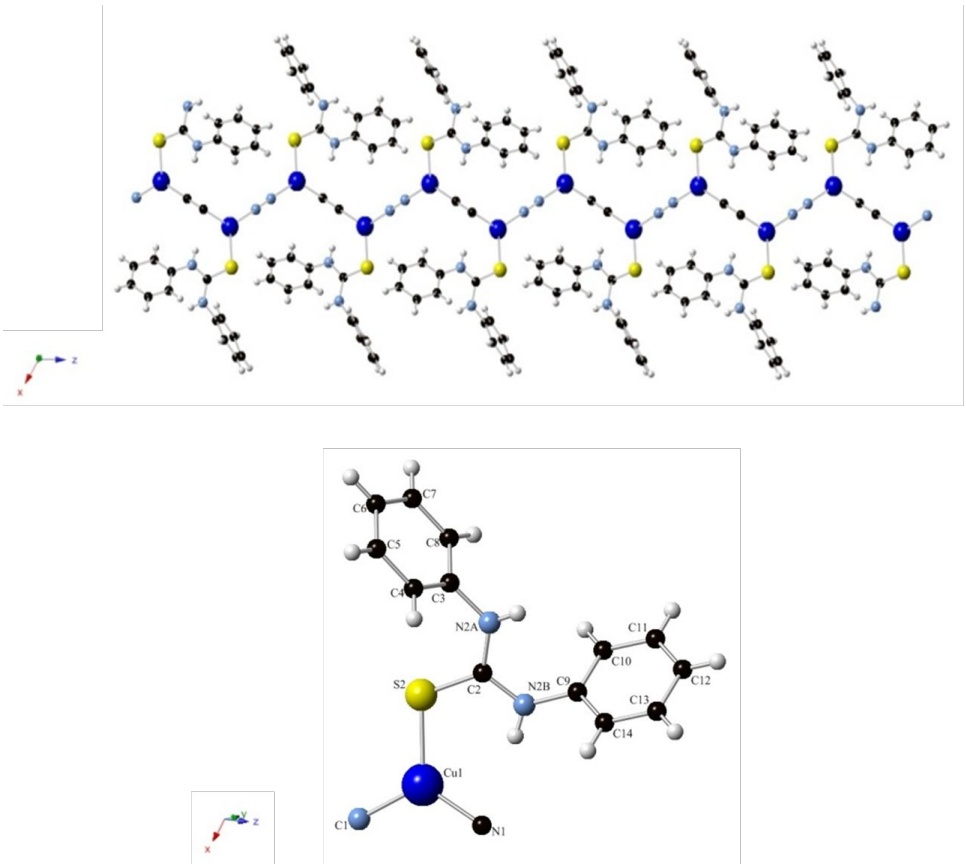

Figure 3. XRSCD structure of **[CuCN(dptu)]$_n$**: **a)** 1D coordination polymer along a axis; **b)** asymmetric unit.

The structure of **[(CuCN)$_3$(fptu)$_2$]$_n$** is a 2D coordination polymer based on bridging cyanides and on μ_2-fptu ligands which form layers (**Figure 4a**). This is the first structure reported with the fptu ligand and Cu(I) or Ag(I) cations. Interestingly, **[(CuCN)$_3$(fptu)$_2$]$_n$** and **[CuCN(dptu)]$_n$** are rare examples where bulky thioureas form coordination polymers, rather than complexes, by adopting a μ_2 coordination mode typical of non-substituted thioureas.[38] The layers are characterized by three non-equivalent Cu(I) cations, namely Cu1 and Cu2 in a trigonal planar environment (SC_2 and SCN, respectively), and Cu3 in tetrahedral coordination (S_2N_2).

The first independent fptu acts as a bridge between Cu1 and Cu2, whereas the second one forms the typical Cu_2S_2 lozenge group with Cu3 (**Figure 4**), with asymmetrical bonds generated by an inversion centre (Cu3–S4=2.341(1) Å and Cu4–S4'=2.544(1) Å). The aromatic rings of the two substituted thioureas form torsion angles on the bonds C12–N4B and C6–N5B of 66.30(12)° and 67.68(15)°, thus implying the absence of intramolecular conjugation between the phenyl ring and the C=S bond. The layers are formed by antiparallel Cu–CN–Cu chains, an arrangement already observed for $(CuCN)_2(L)_3 \cdot H_2O$ (L: N,N'-diethylthiourea),[17] which are bound by alternating single and double sulfur bridges. Three different Cu rings can be observed in the structure: four-atom squares, six-atom hexagons and eight-atom octagons. The significantly different maximum widths of these rings affect the positions of the fptu phenyls: in the Cu8 rings, the two phenyls interact *via* π-stacking with a distance of 3.819(5) Å between the centroids, with displacement and interplanar angles of 18.16(15)° and 5.53(15)°, respectively.[47] This narrower displacement angle with respect to the ideal one for phenyl groups (20°) can be explained by presence of fluorine substituents, which enhance the fully stacked geometry.[48]An extensive H-bonding network (N–H···F) is observed between fptu ligands of different layers (N4A···F2': 3.025(4) Å, and N5A···F4': 3.084(4) Å). As expected, presence of a stronger acceptor, such as the F atoms, explains why H-bonds with cyanide anions are not detected.[49,50]

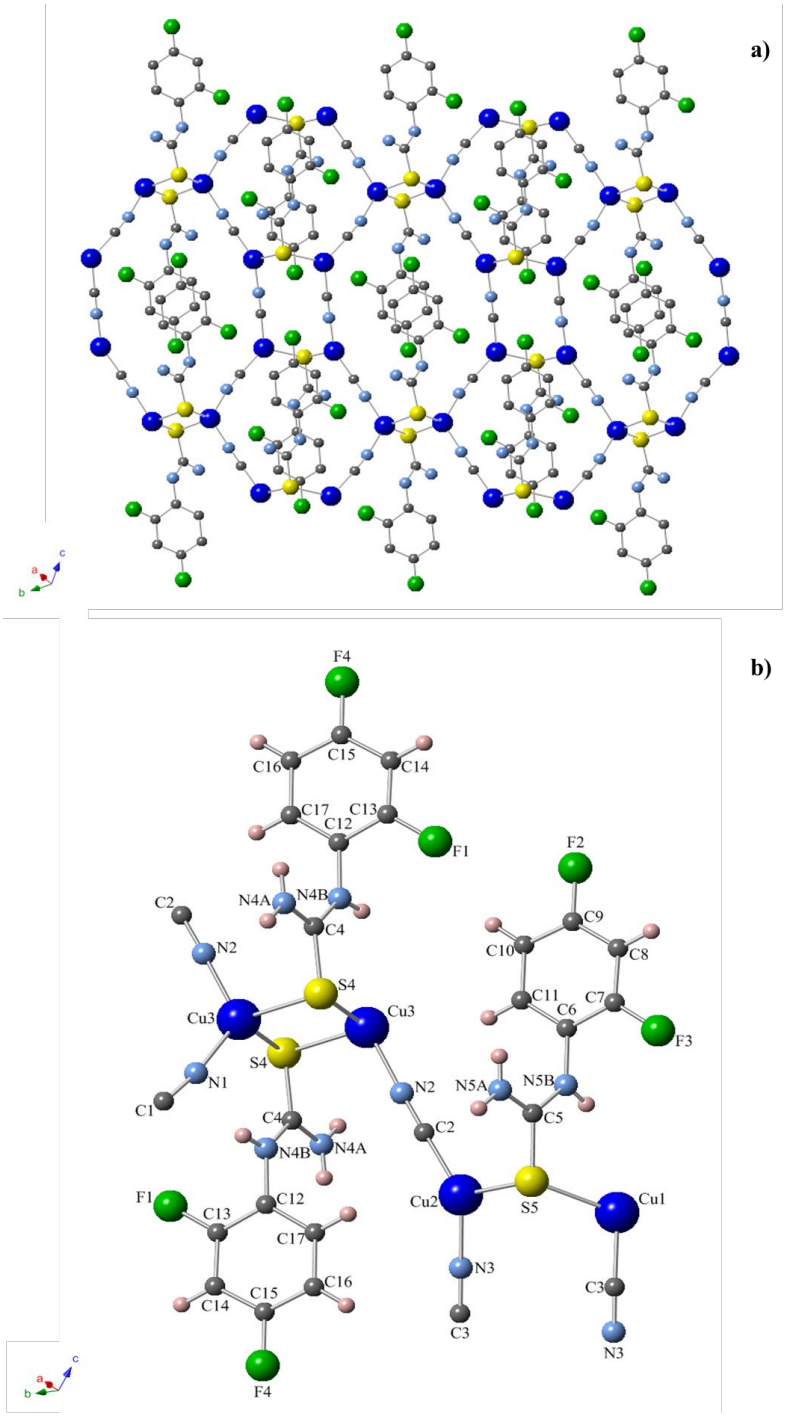

Figure 4. **a)** 2D-polymer in the structure of **[(CuCN)$_3$(fptu)$_2$]$_n$**. For clarity, the hydrogen atoms have been omitted. **b)** The unit that builds the layers. The equivalent fptu presenting a S4 atom and equivalent C2–N2 and C3–N3 cyanides, are generated with –x,–y,–z symmetry code.

Solid State Nuclear Magnetic Resonance. SSNMR characterization was performed for the samples whose seeding experiments were unsuccessful. Although this approach has already been effectively applied to several microcrystalline samples of pharmaceutical crystal forms,[51] it is not yet common for coordination polymers or metal organic frameworks. All SSNMR ^{13}C CPMAS are reported in **Figure 5** while ^{1}H MAS spectra are shown in Figure **S4** in the Supporting Information. Chemical shifts and relative assignments are listed in **Table 2**. The SSNMR spectra of the reagents are reported in the Supporting Information (**Figures S5** and **S6** for ^{13}C CPMAS and ^{1}H MAS, respectively). The NMR interpretation takes advantage of a comparison of the spectra of **[(CuCN)$_2$(tu)]$_n$**, **[CuCN(ptu)]$_n$**, **[CuCN(dptu)]$_n$** and **[(CuCN)$_3$(fptu)$_2$]$_n$** whose structures are known (see above).

The number of ligand molecules in the asymmetric unit can be inferred from the number of ^{13}C signals associated to the same site in the ^{13}C CPMAS spectra (**Figure 5**). The structures of **[(CuCN)$_2$(tu)]$_n$**, **[(CuCN)$_5$(mtu)$_3$]$_n$**, **[(CuCN)$_3$(mtu)$_2$]$_n$**, **[CuCN(ptu)]$_n$**, **[CuCN(dptu)]$_n$** and **[(CuCN)$_3$(fptu)$_2$]$_n$** are characterized by 1, 3, 2, 2, 1, 2 independent ligands in the unit cell, respectively.

The ^{13}C CPMAS spectra show broad signals (in the cases of **[(CuCN)$_2$(tu)]$_n$** and **[(CuCN)$_5$(mtu)$_3$]$_n$** distorted quartets) in the 160–130 ppm range which are attributed to CN. The chemical shift values, similar to that of pure CuCN, point to a bridging coordination mode since a terminal one would have led to low-frequency shifts of about 10–15 ppm.[52] The broadening or the presence of distorted quartets are due to residual dipolar coupling to the quadrupolar nuclei (^{63}Cu and ^{65}Cu), which is not effectively averaged by MAS.[53] Notably, the detection of the CN signal in a CP experiment implies polarization transfer from the organic ligand hydrogen atoms to the CN carbon *via* a dipolar interaction. This is possible only if the CN and the ligand are in

the same unit cell, thus providing evidence of ligand-copper coordination. Cu–S coordination is also clearly confirmed by important low-frequency shifts in the C=S signals, as compared to the pure ligand values, of up to 10.2 ppm in the case of **$[(CuCN)_2(tu)]_n$** (from 181.0 to 170.8 ppm).

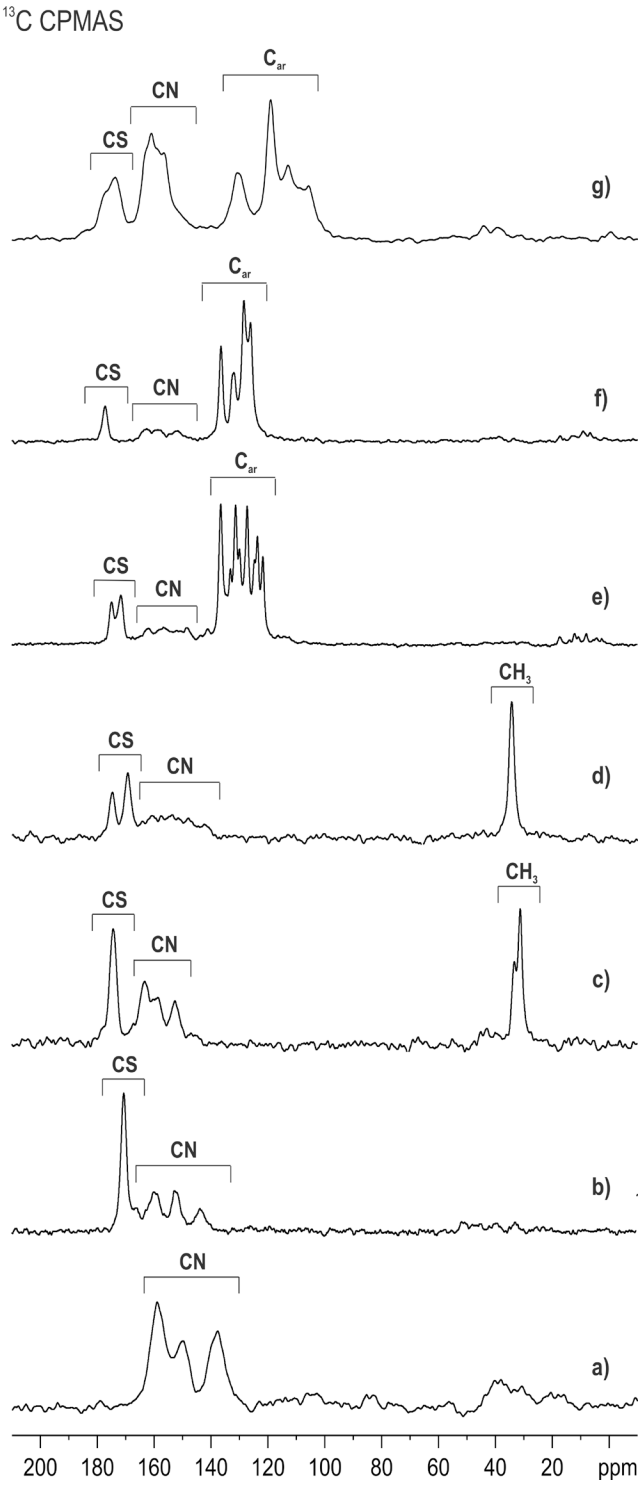

Figure 5. ^{13}C (100 MHz) CPMAS spectra of a) CuCN, b) **[(CuCN)$_2$(tu)]$_n$**, c) **[(CuCN)$_5$(mtu)$_3$]$_n$**, d) **[(CuCN)$_3$(mtu)$_2$]$_n$**, e) **[CuCN(ptu)]$_n$**, f) **[CuCN(dptu)]$_n$** and g) **[(CuCN)$_3$(fptu)$_2$]$_n$** recorded at 12 kHz.

The C=S signals have been assigned for **[(CuCN)$_5$(mtu)$_3$]$_n$** (174.4 ppm), **[(CuCN)$_3$(mtu)$_2$]$_n$** (174.8 and 169.3 ppm), **[CuCN(ptu)]$_n$** (175.1 and 171.8 ppm), **[CuCN(dptu)]$_n$** (177.3 ppm) and **[(CuCN)$_3$(fptu)$_2$]$_n$** (177.6 and 173.9 ppm). The decrease in C=S chemical shifts is proportional to the reduction in the double bond character of C=S, upon Cu–S coordination. Thus, it is related to the lengthening of the C–S distance. For instance, this trend ($\delta_{C=S}$ *vs* C–S distances) is seen in **[(CuCN)$_2$(tu)]$_n$** (170.8 ppm/1.746 Å) and tu (171.8 ppm/1.726 Å, for anhydrous tu; 175.1 ppm/1.714 Å, for the two hydrated forms of tu). Concerning sulfur coordination (terminal or bridging), even though the C=S chemical shift depends on many factors, it generally follows in the footsteps the classical ligand CO.[54] Indeed, we can surmise that **[(CuCN)$_5$(mtu)$_3$]$_n$** is characterized by three equally coordinated mtu while **[(CuCN)$_3$(mtu)$_2$]$_n$** contains two mtu ligands with different coordination modes. Although a general rule on the correlation between C=S chemical shift and coordination mode is not present in literature, we can tentatively suggest that the three equivalent mtu in **[(CuCN)$_5$(mtu)$_3$]$_n$** are more likely characterized by a terminal nature as ligands ($\delta_{C=S}$ = 174.4), whereas in the second one, the two independent mtu moieties are more likely characterized by a terminal nature ($\delta_{C=S}$ = 174.8) and a μ character ($\delta_{C=S}$ = 169.3). A quantitative evaluation of CN groups can also be obtained from SSNMR as confirmed by the comparison between SSNMR and XRSCD results for **[(CuCN)$_2$(tu)]$_n$**, **[CuCN(ptu)]$_n$**, **[CuCN(dptu)]$_n$** and **[(CuCN)$_3$(fptu)$_2$]$_n$**. Thus, the number of CN for **[(CuCN)$_5$(mtu)$_3$]$_n$** and **[(CuCN)$_3$(mtu)$_2$]$_n$**, whose XRSCD structures are not available, could be extracted from the ^{13}C CPMAS with sufficient accuracy although the broadening of the related signals and inherent technical limitations (the CPMAS experiment is not quantitative). An interesting valuation of the weak interactions present in **[(CuCN)$_2$(tu)]$_n$** can be inferred from ^{1}H MAS spectra (**Figure S4** in the Supporting Information) and is also supported by XRSCD

data. Indeed, all four tu hydrogen atoms are involved in weak hydrogen bonds with the CN nitrogen atoms whether they are on the same or different chains (N1B···N3': 3.004(8) Å, N1A···N2: 3.187(8) Å, N1B···N2': 3.243(8) Å, N1A···N3":3.292(8) Å). Thus, the hydrogen bonds weaken on passing from the pure ligand to coordination polymer, as confirmed by the significant low-frequency shift of the ^{1}H NH_2 signals from 8.2–7.0 to 6.5–5.6 ppm.

We observed a low-frequency shift in the resonances attributed to hydrogen-bonded hydrogen atoms in all the other compounds, indicating a weakening of the hydrogen bond in accordance with the covalent nature of the samples. In this sense, **$[CuCN(dptu)]_n$** and **$[(CuCN)_3(fptu)_2]_n$** are exceptions where observed high-frequency shifts are associated to the formation of strong N–H···NC and NH···S interactions, respectively.

Table 2. ^{1}H and ^{13}C chemical shifts (δ) with assignments for all compounds and pure ligands. The number of independent thiourea ligands (Z') is also reported.

Compound	^{13}C	δ [ppm]	^{1}H	δ [ppm]	Z'
tu	**C=S**	181.0	**NH_2**	8.2/7.0	1
$[(CuCN)_2(tu)]_n$	**C=S**	170.8	**NH_2**	6.5/5.6(sh)	1
	C≡N	bb from 160.1 to 144.0			
mtu	**C=S**	179.6/179.2/178.6	**NH_2/NH**	7.7	4
	CH_3	32.3(sh)/32.0/29.8(sh)/29.4	**CH_3**	2.5	
$[(CuCN)_5(mtu)_3]_n$	**C=S**	174.4	**NH_2/NH**	7.5	3
	CH_3	33.5/31.3			
	C≡N	bb from 163.5 to 152.8	**CH_3**	3.0	
$[(CuCN)_3(mtu)_2]_n$	**C=S**	174.8/169.3	**NH_2/NH**	7.2	2
	CH_3	34.2			
	C≡N	164.8/140.1	**CH_3**	3.9(sh)/3.22	
ptu	**C=S**	179.0	**NH_2**	3.2	1
	C_q	136.0	**NH**	4.3	
	CH_{Ar}	133.6/131.4/126.2	**CH_{Ar}**	6.6/9.0^{sh}	
$[CuCN(ptu)]_n$	**C=S**	175.1/171.8	**NH_2/NH**	3.6	2
	C_q	136.7			

	CH_{Ar}	133.3/131.5/130.0/127.4/124.8/123.8/121.8	**CH_{Ar}**	7.0	
	C≡N	bb from 162.4 to 148.5			
dptu	**C=S**	185.4	**NH**	3.1	1
	C_q	140.1	**CH_{Ar}**	6.6	
	CH_{Ar}	132.5/129.7/129.0 (sh)127.9/125.9			
$[CuCN(dptu)]_n$	**C=S**	177.3	**NH**	3.4	1
	C_q	136.5			
	CH_{Ar}	132.6/131.8/128.5/127.2/126.1	**CH_{Ar}**	5.9	
	C≡N	bb from164.8 to 148.7			
fptu	**C=S**	184.9/182.1	**NH_2**	2.5^{sh}	2
	CF	162.5/160.1/157.5	**NH**	6.0	
	C_q	132.1/130.2	**CH_{Ar}**	9.3^{sh}	
	CH_{Ar}	123.8/ 114.8/112.5/106.8			
$[(CuCN)_3(fptu)_2]_n$	**C=S**	177.6/173.9	**NH_2/NH**	3.9/4.6	2
	CF	163.6/161.2159.1156.8			
	C_q	131.0			
	CH_{Ar}	119.2/113.1/109.1/105.9	**CH_{Ar}**	$6.7/8.8^{sh}$	
	C≡N	bb from 187.0 to 146.0			

bb: broad band; sh: shoulder

Infrared Spectroscopy. IR-ATR spectra were principally acquired to screen the progression of the reaction. Particular attention was paid to the 2080–2160 cm^{-1} range, which is typical of bridging cyanide groups.[55] IR-ATR spectra of all the samples prepared are shown in **Figures S7–S12**, while principal assignments are reported in **Table S2** in the Supporting Information. RAMAN characterization was suitable only for **$[(CuCN)_2(tu)]_n$** because the luminescence of the other compounds produces a very broad single band that covers all the signals. As shown in literature, CN stretching modes generally appear in the 2080–2160 cm^{-1} range for typical bridging cyanide groups, while terminal CN groups lead to stretching bands around 2050 cm^{-1}.[56,57] In the studied compounds, ν(CN) bands are observed around 2091–2147 cm^{-1}, confirming the bridging nature of the cyanide groups and the coordination polymer structure of all the samples.

Scheme 2. Different coordination modes of tu with metals.

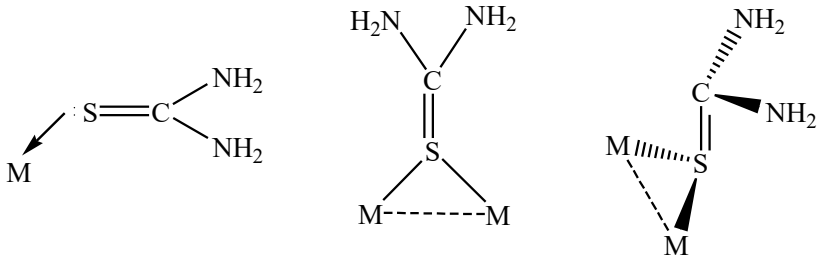

a) b) c)

Its bidentate nature means that tu can coordinate to transition metals through the sulfur or nitrogen. Different coordination modes can be described for sulfur, as depicted in **Scheme 2**.[58] Tu can exist in more than one resonance form, as shown in **Scheme 3**. Structures II and III also become significant upon metal coordination. Thus, Cu(I) is usually characterized by a higher affinity for sulfur than for nitrogen atoms. As a consequence of Cu-coordination through the S-atom, C–S stretching modes decrease in frequency, from 775–721 cm^{-1} (R-tu pure) to 768–686 cm^{-1}, according to the reduction in double bond character. Furthermore, NH_2 bending undergoes a significant increase in frequency from 4 to 54 cm^{-1} upon complexation. On the other hand, if N-coordination had occurred, the shift would have been in the opposite direction.[59]

Scheme 3. Resonance structures of tu.

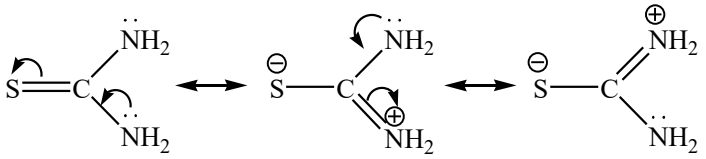

I II III

Pure tu is characterized by a band of medium intensity at 1084 cm^{-1} that can be assigned to NCN stretching,[60] or to a combination of different bands, i.e. ν(CN)+ ν(CS)+ δ(HNC), according to former literature.[61] In the samples under study, this band is characterized by a shift to lower wavenumbers with respect to the pure ligands and shows a decrease of 14 cm^{-1} for **[CuCN(ptu)]$_n$**. NH_2 bending appears at 1606 cm^{-1} for pure tu and in a range from 1590 to 1633 cm^{-1} for all other R-tu. These signals are shifted by 54 cm^{-1} for **[CuCN(dptu)]$_n$** and generally split into 2, 3 or 4 signals in the coordination polymers. The bands above 3100 cm^{-1} correspond to the N–H stretching of the ligands. This is usually split into several bands (in most cases, at higher frequencies, with an increase of about 120 cm^{-1} for **[CuCN(dptu)]$_n$**) after coordination through sulfur with metals (in all cases except for fptu). Indeed, it is characterized by 5 signals (at 3141, 3137, 3171, 3272 and 3361 cm^{-1}) that became two (at 3275 and 3305 cm^{-1}) upon coordination, see **Table S2** in the Supporting Information.

Differential Scanning Calorimetry (DSC) and Thermogravimetric (TGA) Analyses. In order to characterize the thermal behavior and to evaluate the possible presence of adsorbed water molecules in the samples, all compounds were investigated with TGA and DSC. DSC and TGA thermograms of reagents and compounds are reported in **Figures S13–S24** of the Supporting Information, while calorimetric and thermo-gravimetric data are listed in **Table 3**. In general, coordination to a metal leads to an increase in tu ligand thermal stability, as expected. For instance, the melting/decomposition point of **[(CuCN)$_2$(tu)]$_n$** is found around 271.8 °C, while pure tu decomposes at 183.6 °C. In the case of **[(CuCN)$_5$(mtu)$_3$]$_n$** and **[(CuCN)$_3$(mtu)$_2$]$_n$**, the decomposition temperature of ligand increases from 199.8 °C to 216.0 and to 270.7 °C, respectively (ΔT=16.2 and 70.9 °C, respectively). For **[CuCN(dptu)]$_n$**, the melting/decomposition temperature passes from 158.6 (pure dptu) to 168.2 °C (ΔT=9.6 °C). An

exception to this behavior is observed for **[CuCN(ptu)]$_n$** and **[(CuCN)$_3$(fptu)$_2$]$_n$** which show a slight decrease in melting/decomposition temperature in comparison with the corresponding ligands (ΔT=4.3 and 6.4 °C, respectively). All the hydration temperatures are related to a physically adsorbed (not crystallographic) water, as confirmed by XRSCD for **[(CuCN)$_2$(tu)]$_n$**, **[CuCN(ptu)]$_n$**, **[CuCN(dptu)]$_n$** and **[(CuCN)$_3$(fptu)$_2$]$_n$**.

Table 3. TGA and DSC data for **[(CuCN)$_2$(tu)]$_n$**, **[(CuCN)$_5$(mtu)$_3$]$_n$**, **[(CuCN)$_3$(mtu)$_2$]$_n$**, **[CuCN(ptu)]$_n$**, **[CuCN(dptu)]$_n$** and **[(CuCN)$_3$(fptu)$_2$]$_n$**.

Sample	T_w	T_{trans}	T_{fus}	T_{dec}
CuCN	-	185.2, 281.7	453	453
tu	-	146.5	172.6	183.6
[(CuCN)$_2$(tu)]$_n$	-	191.8	271.8	271.8
mtu		-	125.3	199.8
[(CuCN)$_5$(mtu)$_3$]$_n$	65.3, 111.8	131.0	216.0	216.0
[(CuCN)$_3$(mtu)$_2$]$_n$	-	211.4	270.7	270.7
ptu	-	-	171.1	171.1
[CuCN(ptu)]$_n$	-	143.1, 154.9	166.8	166.8
dptu	-	-	158.6	158.6
[CuCN(dptu)]$_n$	68.6, 111.3	-	168.2	168.2
fptu	-	-	176.6	176.6
[(CuCN)$_3$(fptu)$_2$]$_n$	70.1, 112.4	-	170.2	170.2

T_w: dehydration temperature; T_{trans}: polymorphic transition; T_{fus}: melting temperature; T_{dec}: decomposition temperature

Luminescence Measurements. As already reported in the literature, CuCN shows luminescence emission at 392 nm in the solid state.[9,10] This results from electronic excitation between π character orbitals, in particular from the dCu/πCN HOMO to the pCu/π*CN LUMO.[8] After the coordination of amine ligands, the emission of CuCN shifts towards the visible region and two emission pathways become significant: metal to CN and metal to amine. The metal centered (MC) emission pathway seems to be negligible.[62]

The emission and excitation spectra of the studied compounds are reported in **Figure 6**, while the corresponding data are listed in **Table 4** together with the emission lifetimes. Pictures of the samples under visible and UV light (365 nm) are displayed in **Figure 7**. All the coordination polymers exhibit significant luminescence behavior. They all show a broad excitation feature in the 250–350 nm range which is similar to the one displayed by the parent CuCN. However, their luminescence is greatly enhanced when compared with that of CuCN and the other starting materials, such as the aromatic ligands ptu, dptu and fptu that are characterized by very weak emissions around 450 nm (**Figure S25** and **Table S3** in the Supporting Information).

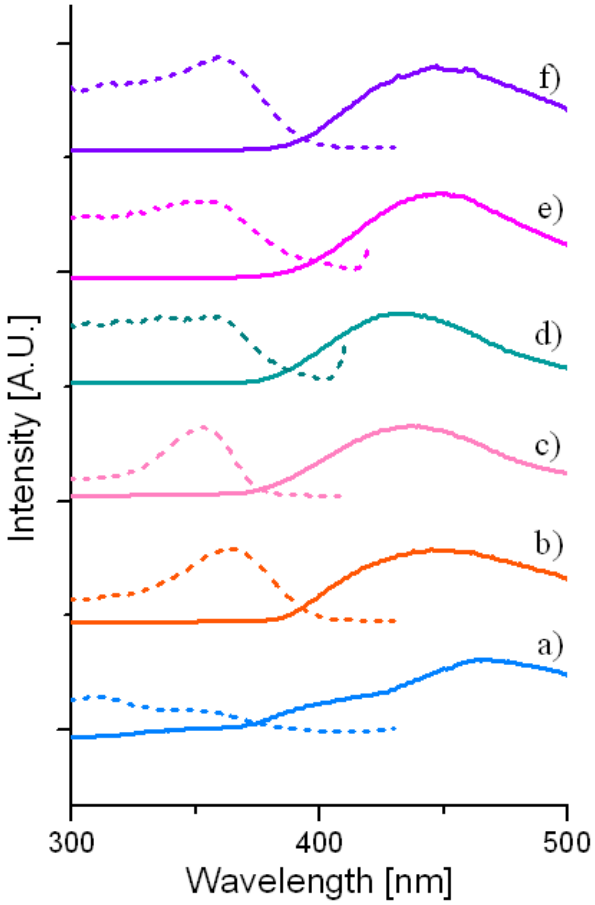

Figure 6. Luminescence emission (solid line) and excitation (dotted line) spectra of a) **[(CuCN)$_2$(tu)]$_n$**, b) **[(CuCN)$_5$(mtu)$_3$]$_n$**, c) **[(CuCN)$_3$(mtu)$_2$]$_n$**, d) **[CuCN(ptu)]$_n$**, e) **[CuCN(dptu)]$_n$** and f) **[(CuCN)$_3$(fptu)$_2$]$_n$**.

Table 4. Luminescence data for **[(CuCN)$_2$(tu)]$_n$**, **[(CuCN)$_5$(mtu)$_3$]$_n$**, **[(CuCN)$_3$(mtu)$_2$]$_n$**, **[CuCN(ptu)]$_n$**, **[CuCN(dptu)]$_n$** and **[(CuCN)$_3$(fptu)$_2$]$_n$**.

Compound	Excitation λ_{max} [nm]	Emission λ_{max} [nm]	Stokes shift [cm^{-1}]	φ	τ [μs]
[(CuCN)$_2$(tu)]$_n$	350	398, 465	3445, 7066	<0.01	17.7
[(CuCN)$_5$(mtu)$_3$]$_n$	363	448	5227	0.19	7.8
[(CuCN)$_3$(mtu)$_2$]$_n$	352	436	5473	0.033	2.9
[CuCN(ptu)]$_n$	355	433	5074	0.082	2.9
[CuCN(dptu)]$_n$	358	448	5611	0.030	2.8
[(CuCN)$_3$(fptu)$_2$]$_n$	360	449	5505	0.12	3.2

φ: quantum yields; τ: lifetimes

After excitation with UV-light, all the coordination polymers display a broad unstructured emission band in the 400–500 nm range, which is assigned to a MLCT (Metal to Ligand Charge Transfer) excited state. The Stokes' shifts are of the order of 5000 cm^{-1} or greater and in agreement with such an assignment. All the compounds, with the exception of **[(CuCN)$_2$(tu)]$_n$**, exhibit significant emission quantum yields, with values ranging from 3.0 to 20 %. The lifetime of the emissive excited state falls in the microsecond range for all compounds and is about 2 orders of magnitude greater than the lifetime of CuCN (nanosecond order).

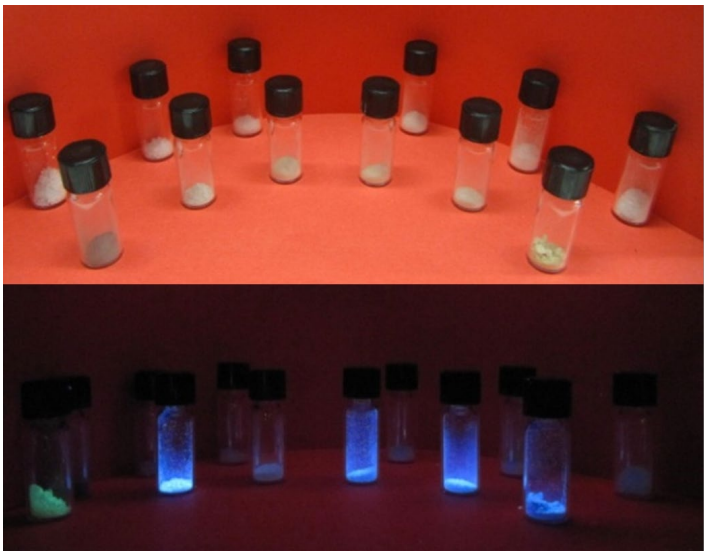

Figure 7: Pictures of powdered samples: from left to right, **$[(CuCN)_2(tu)]_n$**, **$[(CuCN)_5(mtu)_3]_n$**, **$[(CuCN)_3(mtu)_2]_n$**, **$[CuCN(ptu)]_n$**, **$[CuCN(dptu)]_n$** and **$[(CuCN)_3(fptu)_2]_n$** and backward corresponding ligands tu, mtu, mtu, ptu, dptu and fptu under visible light (**a**) and under 365 nm light (**b**).

CONCLUSIONS

In summary, we have described the synthesis and characterization of six new coordination polymers based on copper(I) and thioamide derivatives The compounds were obtained employing both solvent free (mechanochemistry) and solvothermal methods. The former is a reliable alternative with several advantages inherent to the higher reaction yield achieved and to the more environmentally friendly approach.

The structural caracterization of four of the six compounds (**$[(CuCN)_2(tu)]_n$, $[CuCN(ptu)]_n$, $[CuCN(dptu)]_n$** and **$[(CuCN)_3(fptu)_2]_n$**) was achieved by XRSCD while the microcrystalline nature of **$[(CuCN)_5(mtu)_3]_n$** and **$[(CuCN)_3(mtu)_2]_n$** required a combined

approach, based on several solid-state techniques (mainly SSNMR and elemental analysis). In this regard, SSNMR was fundamental to uncover the structural information (independent molecules, copper coordination modes, weak interactions…) of the compounds for which the seeding crystallization experiments were unsuccessful. The thermal stabilities of the ligands were generally improved, increasing up to 88 °C in the case of **[(CuCN)$_2$(tu)]$_n$** over pure tu. The characterization of the structural and electronic properties of all the samples was completed using other techniques (IR-ATR and DR-UV-Vis spectroscopy, XRPD, DSC and TGA analyses). The results are consistent with elemental analysis data. The light-emission properties of all the coordination polymers were investigated in detail, recording not only the emission and excitation spectra but also evaluating the luminescence quantum yields and lifetimes at the solid state. The latter two properties are especially relevant when judging the potential performance for applications.[63] The compounds display emissions in the 398–465 nm range, with significant Stoke's shifts of up to 7066 cm^{-1}. Moreover, emission quantum yield measurements resulted in excellent values ranging from 3.0 to 20 %. An increasing emissive excited state lifetime (2 orders of magnitude greater than the lifetime of CuCN which is of the order of nanoseconds) for all compounds could be inferred. This promising luminescent behavior opens up possible applications for these compounds as sensing molecular devices or OLEDs (Organic light Emitting Diodes).[64] Indeed, unlike conventional light sources, OLEDs offer a wide variability in design possibilities. The shape-optimization of these materials can lead to thin films, flexible sheets or thin wires and so on. Furthermore, the optimization of costs is an outstanding challenge, which can favor the applicability of these materials.

ACKNOWLEDGMENTS:

We are indebted to Prof. L. Celi for the elemental analyses.

ASSOCIATED CONTENT

Supporting Information. Additional spectroscopic and calorimetric data for all compounds: table with bond and angle values and structural data, table with luminescence emission data, figures with asymmetric units and thermal ellipsoid, experimental and calculated XRPD patterns, ^{1}H MAS spectra of all compounds, ^{13}C CPMAS and ^{1}H MAS spectra of the free ligands, IR-ATR spectra, calorimetric and thermogravimetric curves, luminescence spectra of all reagents. This material is available free of charge *via* the Internet at http://pubs.acs.org.

AUTHOR INFORMATION

Corresponding Authors

*E-mail: michele.chierotti@unito.it. Tel: +39011-6707523

roberto.gobetto@unito.it. Tel: +39011-6707520

ABBREVIATIONS

SSNMR, Solid State Nuclear Magnetic Resonance; **DSC**, Differential Scanning Calorimetry; **TGA**, Thermo-Gravimetric Analysis; **XRPD**, X-Ray Powder Diffraction, **XRSCD**, X-Ray Single Crystal Diffraction; **tu**, thiourea; **mtu**, N-methylthiourea; **ptu**, N-phenylthiourea; **dptu**, N,N'-diphenylthiourea; **fptu**, 2,4-difluorophenylthiourea.

REFERENCES

[1]Batten, S. R.; Champness, N. R.; Chen, X. M.; Garcia-Martinez, J.; Kitagawa, S.; Öhrström, L.; O'Keeffe, M.; Suhh, M. P.; Reedijk, J. *CrystEngComm* **2012**, *14*, 3001–3004.
[2]Ropp, R. C. "*Luminescence and the Solid State*", Elsevier, Amsterdam, **2004**.
[3]Miller, K. M.; McCullough, S. M.; Lepekhina, E. A.; Thibau, I. J.; Pike, R. D.; Li, X.; Killarney, J. P.; Patterson, H. H. *Inorg. Chem.* **2011**, *50*, 7239–7249.
[4]Sahu, J.; Ahmad, M.; Bharadwaj, P. K. *Cryst. Growth Des.* **2013**, *13*, 2618–2627.
[5]Yang, X.; Jones, R. A.; Huang, S. *Coord. Chem. Rev.* **2014**, *273,* 63–75.
[6]Ramya, A. R.; Sharma, D.; Natarajan, S.; Reddy, M. L. P. *Inorg. Chem.* **2012**, *51*, 8818–8826.
[7]Decadt, R.; Van Hecke, K.; Depla, D.; Leus, K.; Weinberger, D.; Van Driessche, I.; Van Der Voort, P.; Van Deun, R. *Inorg. Chem.* **2012**, *51*, 11623–11634.
[8]Bayse, C. A.; Brewster, T. P.; Pike, R. D. *Inorg. Chem.* **2009**, *48*, 174–182.
[9]Tronic, T. A.; deKrafft, K. E.; Lim, M. J.; Ley, A. N.; Pike, R. D. *Inorg. Chem.* **2007**, *46*, 8897–8912.
[10]Lim, M. J.; Murray, C. A.; Tronic, T. A.; Dekrafft, K. E.; Ley, A. N.; Debutts, J. C.; Pike, R. D.; Lu, H. Y.; Patterson, H. H. *Inorg. Chem.* **2008**, *47*, 6931–6947.
[11]Korzeniak, T.; Stadnicka, K.; Pełka, R.; Bałanda, M.; Tomala, K.; Kowalski, K.; Sieklucka, B. *Chem. Comm.* **2005**, *23*, 2939–2941.
[12]Bala, M. D.; N. J. Coville, *J. Organomet. Chem.* **2007**, *692*, 709–730.
[13]Cheung, E. Y.; Kitchin, S. J.; M. Harris, K. D.; Imai, Y.; Tajima, N.; Kuroda, R. *J. Am. Chem. Soc.*, **2003**, *125*, 14658–14659.
[14]Friscic, T.; Reid, D. G.; Halasz, I.; Stein, R. S.; Dinnebier, R. E.; Duer, M. J. *Angew. Chem. Int. Ed.* **2010**, *49*, 712–715.
[15]Friscic, T.; Trask, A. V.; Jones, W.; Motherwell, W. D. S. *Angew. Chem. Int. Ed.* **2006**, *45*, 7546–7550.
[16]Le Natur, F.; Calvez, G.; Daiguebonne, C.; Guillou, O.; Bernot, K.; Ledoux, J.; Le Pollès, L.; Roiland, C. *Inorg. Chem.* **2013**, *52*, 6720–6730**.**
[17]Stocker, F. B.; Troester, M. A.; Britton, D. *Inorg. Chem.* **1996**, *35*, 3145–3153.
[18]Heine, J.; Muller-Buschbaum, K. *Chem. Soc. Rev.* **2013**, *42*, 9232–9242.
[19]Cui, Y.; Yue, Y.; Qian, G.; Chen, B. *Chem. Rev.* **2012**, *112*, 1126–1162.
[20]Cinčić, D.; Friščić, T.; Jones, W. *J. Am. Chem. Soc.***2008**, *130*, 7524–7525.
[21]Friščić, T. *Chem. Soc. Rev.* **2012**, *41*, 3493–3510.
[22]Friščić, T.; Jones, W. *Cryst. Growth Des.* **2009**, *9*, 1621–1637.
[23]Bergfors, T. *J. Struct. Biol.* **2003**, *142*, 66–76.
[24]Beckmann, W.; Nickisch, K.; Budde, U. *Org. Proc. Res. Dev.* **1998**, *2*, 298–304.
[25]Agilent Technologies UK Ltd., Oxford, U.K.
[26]Agilent Technologies (20129.CrysAlisPro Software system, version 1.171.35.11, Agilent Technologies U.).
[27]Sheldrick, G. M. SHELXTL, **1997**, Göttingen, Germany.
[28]Flack, H. D. *Acta Crystallogr.* **1983**, *A39*, 876–881.
[29]Flack, H. D.; Schwarzenbach, D. *Acta Crystallogr.* **1988**, *A44*, 499–506.
[30]Antzutkin, O. N.; Shekar, S. C.; Levitt, M. H. *J. Magn. Reson. Ser. A* **1995**, *115*, 7–19.
[31]Antzutkin, O. N.; Lee, Y. K.; Levitt, M. H. *J. Magn. Reson*. **1998**, *135*, 144–155.
[32]Gash, A. G.; Griffith, E. H.; Spofford, W. A.; Amma, E. L. *J.C.S. Chem. Comm.* **1973**, 256–257.
[33]Lobana, T. S.; Sharma, R.; Hundal, G.; Butcher, R. J. *Inorg. Chem.* **2006**, *45*, 9402–9409.
[34]Jia, L.; Kong, L.; Li, D. *Acta Crystallogr.* **2008**, *E64*, m763–m763
[35]Ahmad, S.; Altaf, M.; Stoeckli–Evans, H.; Rüffer, T.; Lang, H.; Mufakkar, M.; Waheed, A. *J. Chem. Crystallogr.* **2010**, *40*, 639–645.
[36]Zouihiri, H. *Acta Crystallogr.* **2012**, *E68*, m260–m261.
[37]Jia, D.; Zhu, A. M.; Ji, M.; Zhang, Y. *J. Coord. Chem.*, **2008**, *61*, 2307–2314.

[38]Bowmaker, G. A.; Hanna, J. V.; Pakawatchai, C.; Skelton, B. W.; Thanyasirikul, Y.; White, A. H. *Inorg. Chem.* **2009**, *48*, 350–368.
[39]Taylor, I. F.; Weininger, M. S.; Amma, E. L. *Inorg. Chem.* **1974**, *13*, 2835–2842.
[40]Johnson, K.; Steed, J. W. *J. Chem. Soc. Dalton Trans.* **1998**, 2601–2602.
[41]Lobana, T. S.; Sharma, R.; Butcher, R. J. *Z. Anorg. Allg. Chem.* **2008**, *634*, 1785–1790.
[42]Crumbliss, A. L.; Gestaut, L. J.; Rickard, R. C.; McPhail, A. T. *J. Chem. Soc., Chem. Commun.* **1974**, 545.
[43]Bowmaker, G. A.; Pakawatchai, C.; Saithong, S.; Skelton, B. W.; White, A. H. *Dalton Trans.* **2010**, *39*, 4391–4404.
[44]Li, D.; Sun, Y.; Liu, S.; Hua, Z. *J. of Coord. Chem* .**2006**, *59*, 403–408.
[45]Desiraju, G. R.; Steiner,T. "*The weak Hydrogen Bond in Structural Chemistry and Biology*", Oxford University Press, New York, **1999**.
[46]Zhu, H. G.; Chen, X. M.; Ng, S. W. *Acta Crystallogr. C* **2000**, *56*, e430–e431.
[47]Janiak, C. *J. Chem. Soc., Dalton Trans.***2000,** 3885–3896.
[48] Hunter, C. A.; Lu, X. J.; Kapteijn, G. M.; van Koten, G. *J. Chem. Soc. Faraday Trans.* **1995**, *91*, 2009–2015.
[49]Howard, J. A. K.; Hoy, J. V.; O'Hagan, D.; Smith, G. T. *Tetrahedron* **1996**, *52*, 12613–12622.
[50]Reichenbächer, K.; Süss, H. I.; Hulliger, J. *Chem. Soc. Rev.* **2005**, *34*, 22–30.
[51]Gaglioti, K.; Chierotti, M. R.; Grifasi, F.; Gobetto, R.; Griesser, U.; Hasa, D.; Voinovich, D. *CrystEngComm* **2014**, *16*, 8252–8262.
[52]Mock, M. T. "*Synthesis and Reactivity of Thioether-supported Organoiron and Low-valent Iron Complexes and Cyanide-bridged Binuclear Complexes*", ProQuest, **2007**.
[53]Kroeker, S.; Wasylishen, R. E.; Hanna, J. V. *J. Am. Chem. Soc.* **1999,** *121,* 1582**–**1590.
[54] Werner, H.; Leonhard, K. *Angew. Chem. Int. Ed.* **1979**, *18*, 627–628.
[55]Nakamoto, K. "*Infrared and Roman Spectra of Inorganic Coordination Compounds"*, Wiley, New York, **1986**.
[56]He, X. *Eur. J. Inorg. Chem.* **2006**, *12*, 2491–2503.
[57]Bowmaker, G. A.; Limb, K. C.; Skelton, B. W.; White, A. H. *Z. Naturforsch* **2004**, *59*, 1264–1276.
[58]Shafique, A.; Anvarhusein, I.; Saeed, A. *J. Coord. Chem.***2003**, *56*, 1587–1595.
[59]Saeed, A.; Isab, A. A.; Perzanowski, H. P. *Transition Metal Chem.* **2002**, *27*, 782–785.
[60]El-Etri, M. M.; Scovell, W. M. *Inorg. Chim. Acta* **1991**, *187*, 201–206.
[61]Mal'kova, T. A.; Shafranskii, V. N. *J. Phys. Chem*. **1975**, *49*, 1653–1653.
[62]Ley, A. N.; Dunaway, L. E.; Brewster, T. P.; Dembo, M. D.; Harris, T. D.; Baril-Robert, F.; Li, X.; Patterson, H. H.; Pike, R. D. *Chem. Commun.* **2010**, *46*, 4565–4567.
[63]Heine, J.; Müller-Buschbaum, K. *Chem. Soc. Rev.* **2013**, *42*, 9232–9242.
[64]Behzad, S. K.; Najafi, E.; Amini, M. M.; Tadjarodi; A.; Dehghani, A.; Notash, B. *Monatsh. Chem.* **2015**, *146*, 35–45.

For Table of Contents Use Only

Solvent-free synthesis of luminescent copper(I) coordination polymers with thiourea derivatives

F. Grifasi,[†] M. R. Chierotti,[*,†] C.Garino,[†] R. Gobetto,[*,†] E. Priola,[†] E. Diana[†] and F.Turci[†]

[†] University of Torino, Department. of Chemistry, and NIS Centre of Excellence Via Pietro Giuria 7, 10125, Turin, Italy

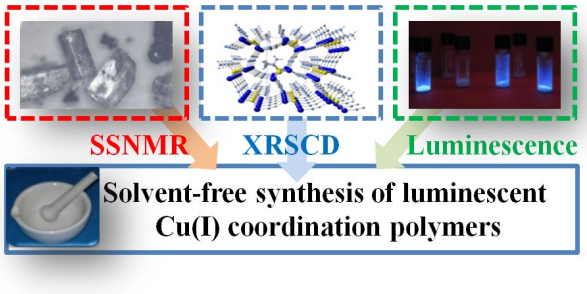

This communication relies on the solvent-free synthesis and characterization of a series of luminescent CuCN based coordination polymers. Their characterization was based on SCXRD, SSNMR, IR, PXRD, DSC and TGA. The properties have been explored recording emission /excitation spectra, and also evaluating quantum yields and lifetimes, uncommon measurements at the solid state, giving promising results for applications as luminescent sensors.